liquids

MDPI

Article

Application of Reichardt's Solvent Polarity Scale ($E_T(30)$) in the Selection of Bonding Agents for Composite Solid Rocket Propellants

Franco Cataldo

Actinium Chemical Research, Via Casilina 1626A, 00133 Rome, Italy; franco.cataldo@fastwebnet.it

Abstract: Bonding agents (BA) are key compounding ingredients for the correct formulation of composite solid rocket propellants (CSRP). In particular, the addition of BA is essential to achieve suitable mechanical properties of CSRP in terms of adequate tensile strength and elongation at the break. It is shown that the polarity of each conventional BA as well as new potential BA can be measured through the Reichardt's $E_T(30)$ polarity scale. Using this methodology, it was possible to propose a substitute for MAPO (tris-(methylaziridinyl)-phosphine oxide), a conventional BA with the drawback of high toxicity and high reactivity, with TTPT (tris-(pyrrolidine)-phosphine oxide), a completely safe and effective BA. In this work, several other potential BA were evaluated through the Reichardt's $E_T(30)$ polarity scale but only a selection of the potential BA were effectively tested in a standard CSRP. The evaluation of TTPT vs. MAPO showing the ability of the former BA to match the mechanical properties of the latter BA was particularly interesting. A reasonable correlation between the elongation at break of the CSRP and the $E_T(30)$ value of the BA used in the compound was found.

Keywords: bonding agents (BA); composite solid rocket propellants (CSRP); Reichardt's $E_T(30)$ polarity scale; mechanical properties of CSRP

check for updates

Citation: Cataldo, F. Application of Reichardt's Solvent Polarity Scale ($E_T(30)$) in the Selection of Bonding Agents for Composite Solid Rocket Propellants. *Liquids* **2022**, *2*, 289–302. https://doi.org/10.3390/liquids2040017

Academic Editors: William E. Acree, Jr. and Enrico Bodo

Received: 31 August 2022
Accepted: 19 September 2022
Published: 27 September 2022

Publisher's Note: MDPI stays neutral with regard to jurisdictional claims in published maps and institutional affiliations.

Copyright: © 2022 by the author. Licensee MDPI, Basel, Switzerland. This article is an open access article distributed under the terms and conditions of the Creative Commons Attribution (CC BY) license (https://creativecommons.org/licenses/by/4.0/).

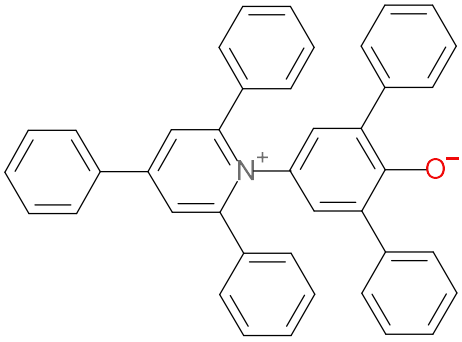
1. Introduction

Composite solid rocket propellants (CSRP) are the typical components of solid rocket motors. CSRP are based on highly filled elastomers matrix or binder and are used as energetic materials for military ordnance and rockets propulsion. As lively accounted by Mason and Roland (1), the actual standard formulation of solid composite propellants consists of hydroxyl-terminated polybutadiene (HTPB) (8–10%), an isocyanate crosslinker (1–2%), a crosslinking catalyst (0.1%), a plasticizer (0–10%), the oxidizer (60–90%), metal powder (0–20%), a bonding agent (1%), burn rate modifier (1%), and an antioxidant (0.1%). The standard oxidizer is currently the ammonium perchlorate (AP) while the preferred metal is aluminum [1–3]. Of course, many new binders and oxidizers are becoming available [1–5], but the HTPB-based technology remains the current standard CSRP [1].

Among the mentioned compounding ingredients of a CSRP, the bonding agents (BA) are special and critical additives. The BA play a very critical role as compatibilizers between the crystalline and ionic filler or oxidizer represented for instance by ammonium perchlorate from one side and the apolar polymer matrix (e.g., hydroxyl-terminated polybutadiene = HTPB) [2]. Although the BA are added into the propellant formulation in relatively small amounts, they lead to significant improvements in the propellant mechanical properties in terms of tensile strength, reducing possible failure risks upon high acceleration and deceleration, i.e., the so-called slumping phenomenon [2,3]. Other functions of the bonding agents regard the reduction in the accidental ignition risk of the solid propellants by counteracting its delamination [2,3]. BA are relatively low molecular weight compounds characterized by the presence of two or more functional groups reactive with the curing agents [3]. Perhaps, the most recent, updated, and comprehensive review on BA is that of Gan et al. [6]. Several classes of BA are

presented and discussed in [6], including novel types of bonding agents and evaluation methods regarding the effectiveness of each BA. One key parameter considered in the evaluation of the effectiveness of a bonding agent regards the tensile strength and the elongation at break of the SRP [1,6]. Additionally, other methods rely on surface tension evaluation [1,6], differential scanning calorimetry [7] and accelerated ageing of the CSRP [8].

This work shows an innovative approach in the evaluation and in the selection of the bonding agents based on the application of Reichardt's solvent polarity scale [9–14]. In particular, Reichardt's empirical solvent polarity scale has already shown its effectiveness and usefulness in different fields and applications of chemistry as reported in ref. [9–14], including ionic liquids, solute–solvent interactions and relative solvatochromism [15], micellar systems [16] and so on. Reichard's solvent polarity scale is based on the use of a dye called (30) which is based on a pyridinium-N-phenolate betaine chemical structure characterized by a charge-separated zwitterion. Scheme 1 shows the structure of Reichardt's dye (30), i.e., of 2,6-diphenyl-4-(2,4,6-triphenyl-1-pyridinio)phenolate or 2,6-diphenyl-4-(2,4,6-triphenylpyridinio)phenolate [9–14].



Scheme 1. Chemical structure of Reichardt's dye (30); it is a pyridinium-N-phenolate betaine dye i.e., 2,6-diphenyl-4-(2,4,6-triphenyl-1-pyridinio)phenolate.

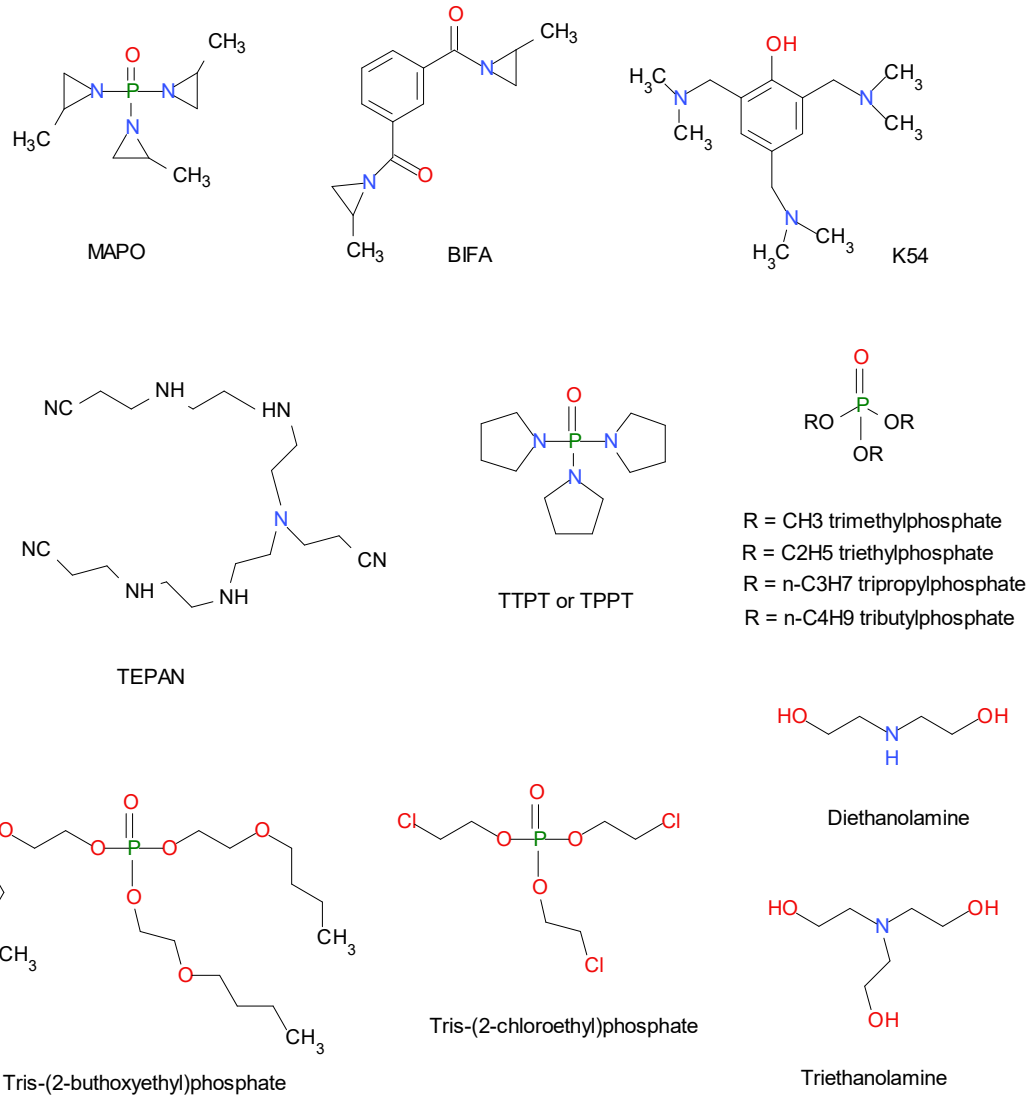
Reichardt's (30) dye acts as a molecular probe once dissolved in a solvent medium. In more detail, Reichardt's dye is a molecule that exhibits a strong and negative solvatochromism, with the largest known hypsochromic shift (blue shift) of its charge-transfer (CT) electronic transition on passing from apolar or less polar liquid medium to high polar liquid. This effect is explained from the fact that the ground state of Reichardt's (30) dye is characterized by a zwitterionic structure with charge separation and a dipole moment of 15 D while the excited state is instead characterized by a lower dipole moment of only 6 D [12]. Thus, the vertical transition to the first excited state results in a significant decrease in the dye polarity since the excited state dipole moment is less than half the value of the ground state. In other words, the solute–solvent interaction which broadly speaking can be visualized by the position of the CT band of the Reichardt's (30) dye, in the excited state interacts better with apolar solvents leading to low energy and long wavelengths electronic transition. In contrast, the Reichardt's (30) dye interaction with polar solvents requires higher energy and hence the CT band is found at shorter wavelengths. The molar transition energies (i.e., E_T) of the (30) betaine dye (hence E_T(30) scale) expressed in kcal/mol have been proposed as empirical parameter for the measurement of solvent and even surfaces polarity [9–11].

Spange et al. [17] made a summary of the physical meanings attributed to Reichardt's solvent polarity scale.

2. Experimental Section

The known BA MAPO (tris-(methylaziridinyl)-phosphine oxide) and K54 as well as BIFA and TEPAN (see Scheme 2 for chemical structures) were commercially available chemicals which were used as received. All the other chemicals used in the present work,

including Reichardt's (30) dye (Scheme 1) were purchased from Merck-Aldrich and used without any further purification.



Scheme 2. Current bonding agent MAPO, i.e., tris-(2-methyl-1-aziridinyl)-phosphine oxide, BIFA (called also HX752), i.e., 1,1-isophthaloyl-bis-(2-methylaziridine), K54 i.e., tris-(2,4,6-dimethylaminomethyl) phenol and TEPAN, i.e., reaction product between tetraethylenepentamine and acrylonitrile; the trial BA tris-(pyrrolidine)-phosphine oxide (TTPT or TPPT), other trial BA trialkylphosphates derivatives (i.e., trimethyl- triethyl- tri-n-propyl- and tri-n-butyl-phosphates, respectively, TMP, TEP, TPP, and TBP) as well as tris-(2-buthoxyethyl)phosphate (TBUOP) and tris-(2-chloroethyl)phosphate (TCEP); two amino-alcohol bonding agents diethanolamine (DEA) and triethanolamine (TEA).

2.1. Typical Measurement Procedure of the Liquid Polarity with Reichardt's Dye

Reichardt's (30) dye displays three main electronic transitions in its UV-VIS spectrum. The first two electronic transitions are not sensitive to the liquid polarity and occur at about 304–309 nm ($\varepsilon \approx 37{,}000$–$46{,}000\ M^{-1}\ cm^{-1}$) and at 374–389 nm ($\varepsilon \approx 9900$–$12{,}000\ M^{-1}\ cm^{-1}$) [12]. Only the longest wavelength electronic transition of Reichardt's (30) dye is characterized by a remarkable solvatochromism from about 400 nm to the threshold of the near infrared spectral window, i.e., at about 850 nm with $\varepsilon \approx 5000$–$7000\ M^{-1}\ cm^{-1}$ [12]. Consequently, in our study on the BA liquids we focused our attention to the latter band, which is due to the intramolecular charge-transfer transition from the HOMO (i.e., from phenolate) to the LUMO (i.e., pyridinium group) [12].

The liquid under study (10 mL) was loaded with the minimum quantity of Reichardt's dye sufficient to reach a reasonably good absorption band in the visible spectral range. The dissolution of Reichardt's dye was achieved by stirring, seldom by gently heating. Since Reichardt's dye is also thermochromic, all measurements were made using quartz cuvettes held in a TCC-100 thermoelectrically temperature-controlled cell-holder maintained at 24 °C on a Shimadzu UV2450 spectrophotometer.

The polarity of each liquid BA studied was evaluated according to the following equations [9–11]:

$$E_T(30) = [28{,}591/\lambda_{max}] \quad \text{(expressed in kcal/mol)} \tag{1}$$

$$E_T(30) = [(28{,}591 \times 4.184)/\lambda_{max}] \quad \text{(expressed in kJ/mol)} \tag{2}$$

The data are reported in Table 1 together with a series of selected $E_T(30)$ values of other representative liquids/solvents which may be considered pertinent to the present work and taken from other sources [10,11]. It is worth remembering here that higher polarity liquids in Reichardt's scale display the most energetic electronic transitions (corresponding to shorter wavelength position of the electronic transition of the dye, i.e., high $E_T(30)$ values), while the opposite reasoning applies to less polar liquids with the dye electronic transition red shifted toward longer wavelengths (leading to lower $E_T(30)$ values).

2.2. Mechanical Properties of HTPB-SRP with Different BA

A selection of BA, including the reference MAPO were mixed with HTPB and AP according to standard conditions [1,4] using the typical SRP formulation essentially disclosed in ref. [1]. The selected formulation was based on hydroxyl-terminated polybutadiene (HTPB) (18%), an isocyanate crosslinker (≈2%), a crosslinking catalyst (0.1%), the AP oxidizer (68%), metal powder (14%), a bonding agent (≈1%), burn rate modifier (1%), antioxidant (0.1%). No plasticizers such as dioctyl adipate and the like were added to the formulation. The usual casting technique was employed to prepare the propellant samples, starting with the mixing of various ingredients with liquid HTPB for 2 h using a 4 kg stainless steel mixer under vacuum followed by the addition of calculated quantity of the diisocyanate and curing catalyst under vacuum. The test specimens were molded into a dumbbell-shaped mold with the JANNAF dimensions [18,19]. The samples were cured for 7 days at 60 °C. The cured samples were tested at the Zwick dynamometer (using a crosshead speed 50 mm/min at +21 °C) to determine the tensile strength and the elongation at break. The data reported are the averaged results of three test specimens for each BA evaluated. A blank, reference sample was prepared without any BA addition, to show the effect of BA on the mechanical properties of the SRP.

Table 1. Summary of the $E_T(30)$ values, dielectric constants (ε_r) and dipole moments (μ) of bonding agents and other liquids.

	λ_{max}; nm	$\tilde{\nu}$; cm^{-1}	$E_T(30)$; kcal/mol	$E_T(30)$; kJ/mol	ε_r; Dielectric Constant	μ; Debye	Notes	Reference
Triethanolamine (TEA)	***534.4***	***18,713***	**53.5**	**223.8**	**29.4**	**3.57**	ref. [10] reports ET(30) = 49.6 kcal/mol	**This work**
Diethanolamine (DEA)	*536.1*	*18,653*	**53.3**	**223.1**	24.0	2.8		**This work**
Tris-(tripyrrolidino)-phosphoric acid triamide (TTPT)	***543.8***	***18,389***	**52.6**	**219.9**	**45.1**	**7.3**	ε and μ from ref. [20] μ = 5.52 D in bz 7.3 D in bulk	**This work**
1,1-Isophthaloyl-bis-(2-methylaziridine) (HX752 or BIFA)	***607.1***	***16,472***	**47.1**	**197.0**				**This work**
Propylene carbonate	*618.5*	*16,168*	**46.2**	**193.4**	66.1	4.9	ref. [10] reports ET(30) = 46.0 kcal/mol	**This work**

Table 1. *Cont.*

	λ_{max}; nm	$\tilde{\nu}$; cm^{-1}	$E_T(30)$; kcal/mol	$E_T(30)$; kJ/mol	ε_r; Dielectric Constant	μ; Debye	Notes	Reference
Dimethyl sulfoxide	*625.0*	*16,000*	**45.7**	**191.4**	47.2	4.0	ref. [10] reports ET(30) = 45.1 kcal/mol	**This work**
Acetonitrile	*627.0*	*15,949*	**45.6**	**190.7**	36.6	3.9		[9–11]
TEPAN (*)	***642.2***	***15,571***	**44.5**	**186.2**				**This work**
Sulfolane	*649.8*	*15,389*	**44.0**	**184.1**	43.3	4.8		[9–11]
Trimethylphosphate (TMP)	*655.7*	*15,251*	**43.6**	**182.4**	20.6	3.2		[9–11]
Tris-(2-chloroethyl)phosphate (TCEP)	*655.4*	*15,258*	**43.6**	**182.5**				**This work**
N,N-Dimethylformamide (DMF)	*661.8*	*15,110*	**43.2**	**180.7**	38.2	3.8		[9–11]
N,N-Dimethylacetamide (DMAC)	*666.4*	*15,006*	**42.9**	**179.5**	38.8	3.8		[9–11]
N-Methyl-pirrolidone (NMP)	*677.5*	*14,760*	**42.2**	**176.5**	32.2	4.1		[9–11]
Tris-(2,4,6-dimethylaminomethyl) phenol (K54)	***682.4***	***14,654***	**41.9**	**175.3**				**This work**
Triethylphosphate (TEP)	*685.6*	*14,586*	**41.7**	**174.4**	13.2	3.08		[9–11]
Benzonitrile	*688.9*	*14,516*	**41.5**	**173.6**	25.2	4.2		[9–11]
Tris-(2-methyl-1-aziridinyl)-phosphine oxide (MAPO)	***691.3***	***14,465***	**41.4**	**173.0**	**14.6**	**3.5**	ε and μ from ref. [21] data on APO	**This work**
Tris-(2-buthoxyethyl)phosphate (TBUOP)	*696.3*	*14,362*	**41.1**	**171.8**				**This work**
Tri-n-propylphosphate (TPP)	*706.0*	*14,165*	**40.5**	**169.4**	10.0	3.75		[9–11]
Hexamethylphosphoramide (HMPA) or Hexamethylphosphoric acid triamide (HMPT)	*699.0*	*14,306*	**40.9**	**171.1**	31.3	5.5	from ref. [10,11] μ = 4.37 in bz and 5.5 in bulk	[9–11]
Hexamethyl phosphorothioic acid triamide (HMPTS)	*723.8*	*13,816*	**39.5**	**165.2**	39.5	4.8	ε and μ from ref. [22]	[9–11]
Tributyl phosphate (TBP)	*728.5*	*13,727*	**39.2**	**164.2**	8.3	3.07		[9–11]
Aziridine or ethylenimine					18.3	1.9		
Diethylamine	*807.6*	*12,382*	**35.4**	**148.1**	3.68	0.92		[9–11]
Trietylamine	*890.7*	*11,227*	**32.1**	**134.3**	2.4	0.66		[9–11]

(*) reaction product between tetraethylenepentamine and acrylonitrile. Bold combined with bold italic character show the BA which were also tested for mechanical properties in CSRP. All data on dielectric constants and electric dipole moment are from ref. [23], unless otherwise stated.

3. Results

3.1. Measurement of $E_T(30)$ Value of Selected Current BA and Potential BA Candidates

Figure 1 shows that the longest wavelength electronic transition of Reichardt's dye in the reference BA MAPO occurred at 691.3 nm. Among the phosphoramides that potentially may replace MAPO, tris-(pyrrolidino)-phosphoric acid triamide (TTPT) was selected in this study (see Scheme 2 for chemical structure and discussion section for further details about this choice). Figure 1 shows that Reichardt's (30) dye dissolved in TTPT showed the longest wavelength transition at 543.8 nm with a considerable hypsochromic shift with respect to that recorded to MAPO. The results are summarized in Table 1 also in terms of $E_T(30)$ scale and clearly suggest a higher polarity for the TTPT with respect to MAPO. These aspects will be discussed more broadly in the next section. It is also curious that TTPT in addition to the neat peak at 543.8 nm also showed a long tail with a shoulder at 728 nm. The product was pure >97% as analyzed by GC and reported by the vendor. However, it is possible that some impurity present in the product yielded the secondary shoulder at 728 nm. The possible source of such secondary transition was most probably due to free pyrrolidine impurity which was used for the synthesis of TTPT. In fact, the $E_T(30)$ value of pyrrolidine was reported [10,11] at 39.1 kcal/mol which corresponded to an electronic transition of Reichardt's dye at 731 nm, in fair agreement with the measured value.

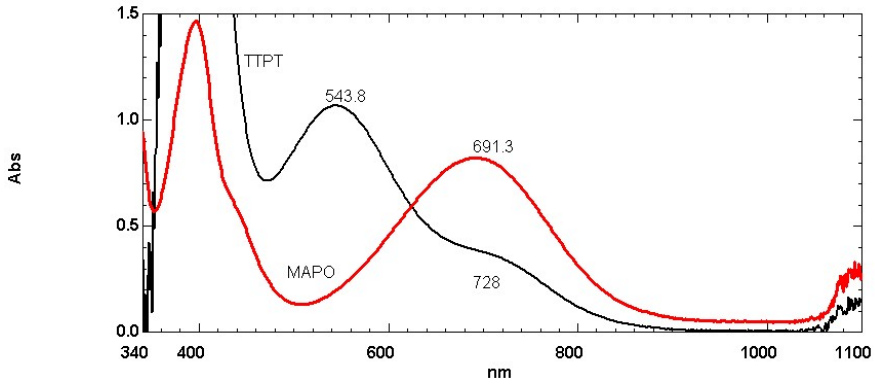


Figure 1. Electronic absorption spectra of Reichardt's (30) dye dissolved in MAPO BA liquid and in the trial BA TTPT (for chemical structures see Scheme 2).

The other three commercially available BA, namely K54 as well as TEPAN and BIFA (see Scheme 2 for chemical structures) were also studied with Reichardt's dye and the resulting electronic absorption spectra are reported in Figure 2. Among these BA, the most energetic electronic transition was shown by BIFA at 607.1 nm, followed by the polyamine TEPAN at 642.2 nm and then K54 with the maximum at 682.4 nm. Moreover, in this case, the electronic transitions of these BA were translated into the $E_T(30)$ scale in Table 1 using Equations (1) and (2).

As new potential BA, in addition to TTPT, a series of alkylphosphates were taken into consideration. The chemical structures of the selected alkylphosphates considered here are shown in Scheme 2. Since the $E_T(30)$ values of simple alkylphosphates such as trimethyl-, triethyl-, and tri-n-propylphosphate were already measured and tabulated [10,11], we focused on the determination of the $E_T(30)$ value of tributylphosphate, tris-(2-buthoxyethyl)-phosphate and tris-(2-chloroethyl)-phosphate. Figure 3 shows longest wavelength transition in the latter three liquids for Reichardt's (30) dye. The results are also reported in Table 1 in terms of $E_T(30)$ values. As heuristically expected, the polarity increased on passing from tributylphosphate to tris-(2-buthoxyethyl)-phosphate and reached the maximum negative solvatochromism on the chlorinated derivative and tris-(2-chloroethyl)-phosphate.

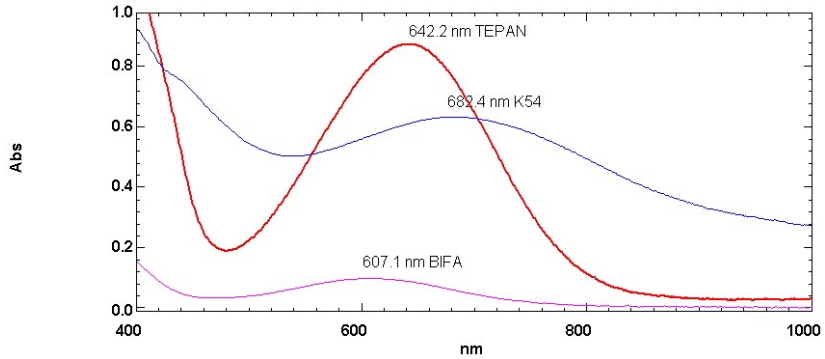


Figure 2. Electronic absorption spectra of Reichardt's dye dissolved in the following BA: TEPAN (red curve), K54 (blue curve) and BIFA or HX752 (pink curve) (for chemical structures see Scheme 2).

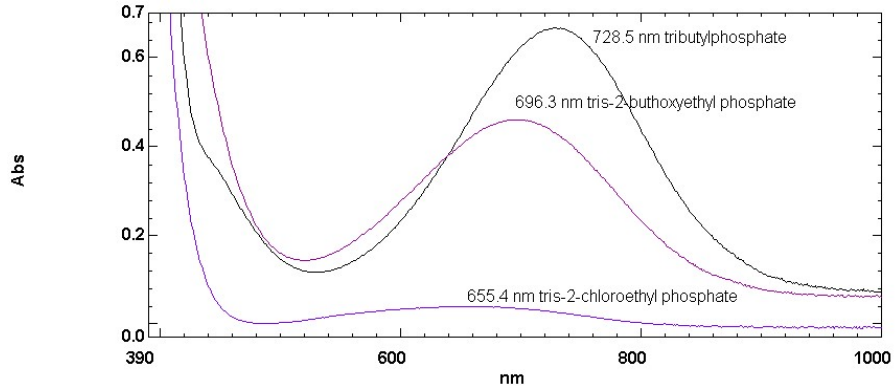


Figure 3. Electronic absorption spectra of Reichardt's dye dissolved in the following liquids: tributylphosphate (black curve), tris-(2-buthoxyethyl)-phosphate (dark pink curve), and tris-(2-chloroethyl)-phosphate (violet curve) (for chemical structures see Scheme 2).

In addition to the phosphates, we also considered in this study the $E_T(30)$ value of diethanolamine and triethanolamine, molecules which have the double functionality alcoholic and amine and belong to the BA class of alcohol-amine [6]. Figure 4 shows the electronic absorption spectra of Reichardt's dye dissolved in these two liquids. Table 1 reports also the corresponding $E_T(30)$ values. As shown in Table 1, our measurement showed a higher $E_T(30)$ value of 53.5 kcal/mol for triethenolamine with respect to the tabulated value of 49.6 kcal/mol reported in ref. [10,11]. Such a value was also measured on diethanolamine with $E_T(30)$ = 53.3 kcal/mol as shown in Table 1.

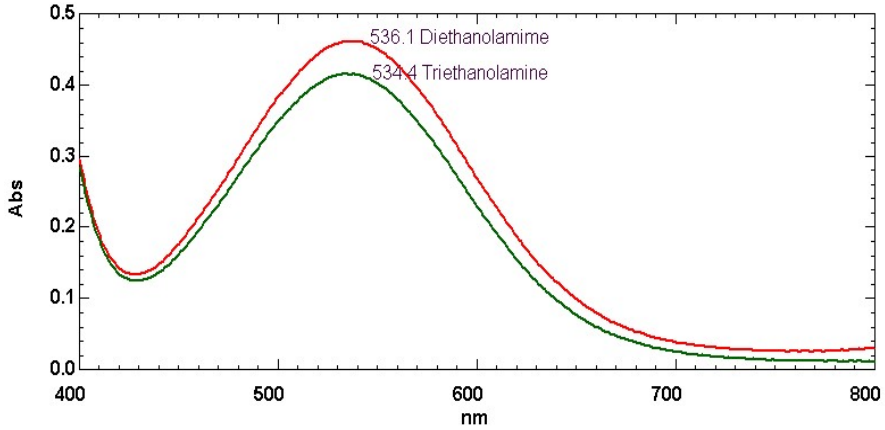


Figure 4. Electronic absorption spectra of Reichardt's dye dissolved in the following liquids: diethanolamine (red curve); triethanolamine (green curve) (for chemical structure see Scheme 2).

3.2. Evaluation of Selected BA in a Standard CSRP

The evaluation of current and potential BA through Reichardt's (30) dye revealed that the higher $E_T(30)$ value was offered by triethanolamine (TEA) followed by the phosphoramide TTPT (see Table 1). Thus, an excellent compatibilization effect between the AP filler and the HTPB binder or matrix exerted by these two potential BA was expected. On the other hand, the current BA such as BIFA (or HX752), TEPAN and K54 were characterized by lower $E_T(30)$ values (47.1, 44.5, and 41.9 kcal/mol, respectively) in comparison to TEA and TTPT (53.5 and 52.6 kcal/mol). It was then decided to evaluate both TEA and TTPT against TEPAN, excluding BIFA since its mechanism of action as BA is different than that of TEPAN and more similar to MAPO. The BA K57 was excluded from the evaluation in CSRP because its considerably lower polarity in the $E_T(30)$ Reichardt's scale and its mechanism of action similar to that of TEA and TEPAN. Conversely, TEPAN can be viewed as somewhat similar in its mechanism of action to that exerted by TEA and TTPT. Finally, MAPO was evaluated in CSRP because it is the absolute reference BA; it has been a standard BA for a long time in CSRP. The evaluation with Reichardt's (30) dye revealed that MAPO was not characterized at all by a specially high polarity, since its $E_T(30)$ = 41.4 kcal/mol was even closer to normal alkylphosphates which indeed were evaluated as well with Reichardt's dye in Table 1. Previously, it was shown that either MAPO and APO were not characterized at by especially high donor number (DN) values [24], a circumstance more firmly confirmed later by other authors [25]. The special or even unique properties of MAPO in terms of mechanism of action with AP has already been discussed elsewhere [6], involving also the ring-opening polymerization of the aziridinyl rings (see also the discussion section).

Figure 5 shows the mechanical properties of a standard CSRP in terms of stress–strain properties. The CSRP compounded without any BA, it is immediately evident the low tensile strength (570 kPa) and the extremely low elongation at break (about 11%), which was due to the complete absence of the interaction between the HTPB binder (crosslinked with isocyanate) and the AP filler also contained Al particles. On the other hand, Figure 5 shows the excellent performances of MAPO, which instead was able to increase considerably the key parameters represented by the tensile strength and the elongation at break, respectively, at 1235 kPa and 27% of the elongation at the break. Definitely, MAPO works well and it is an effective BA. Figure 5 shows that the new candidate BA phosphoramide derivative TTPT also worked as well as MAPO although its mechanism of action did not involve the ring-opening polymerization of the pyrrolidine at all. TTPT gave a tensile strength of about 1200 kPa with an elongation at 30%. These data suggest that TTPT matches in full the performances of MAPO as BA in CSRP with a different mechanism of action and can overcome the great concerns linked to the high toxicity of MAPO.

Figure 5 also shows the performance of TEPAN and TEA in the standard CSRP. These two BA were able to supply higher elongation at break to the CSRP with the drawback of a reduction in tensile strength, which was more severe with the use of TEA. Of course, TEPAN and TEA were confirmed as suitable BA in the hands of the CSRP compounder as a tool to produce especially high elasticity to the CSRP.

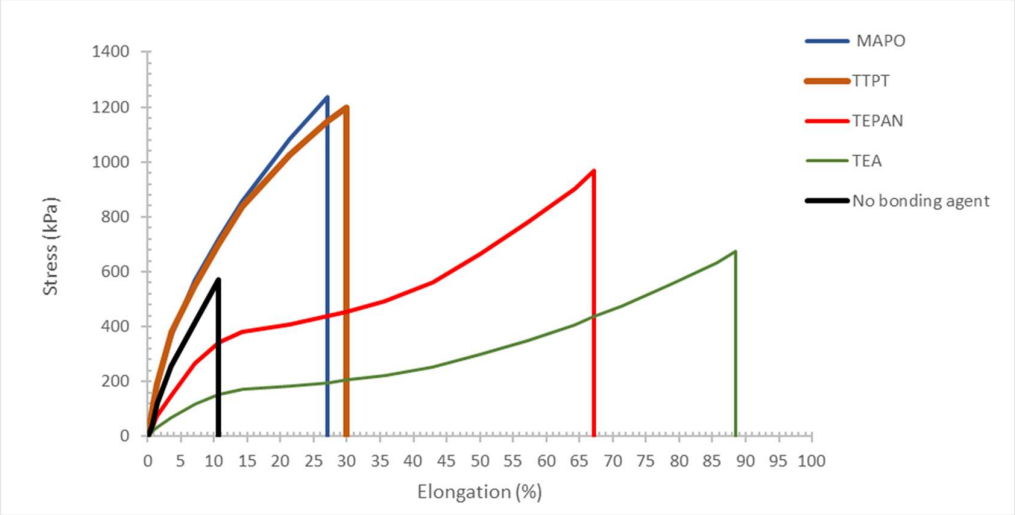
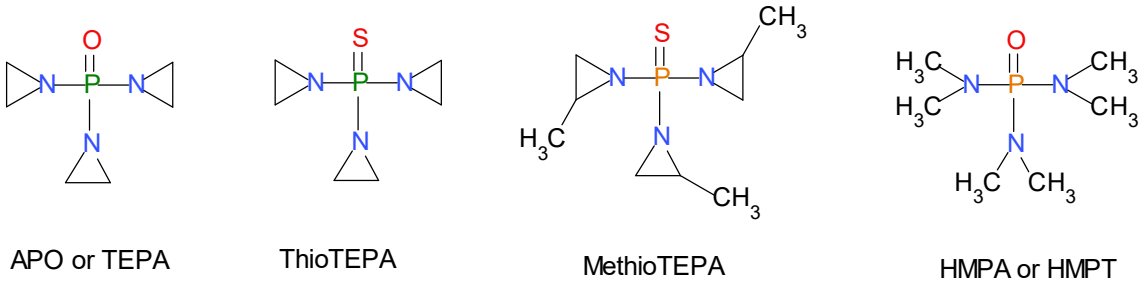


Figure 5. Stress–strain properties of the CSRP standard formulation compounded with 1% of different types of BA. MAPO represents the standard BA (blue trace), also TEPAN can be considered another standard (red trace). It is evident that TTPT (brown trace), proposed as new BA matched the performances of MAPO, while TEA (green trace) was not at the same level of TEPAN in terms of tensile strength (see discussion section form more details). The black trace is an example of SRP standard formulation compounded without BA.

4. Discussion

As already stated in the introduction, the present study focused on a series of common bonding agents (BA) used in standard HTPB-based SRP. In more detail, the conventional bonding agents considered here were MAPO tris-(2-methyl-1-aziridinyl)-phosphine oxide shown in Scheme 2 together with BIFA or HX752 which is 1,1-isophthaloyl-bis-(2-methylaziridine), with K54 bonding agent which is tris-(2,4,6-dimethylaminomethyl) phenol and with TEPAN, i.e., the reaction product between tetraethylenepentamine and acrylonitrile.

Surprisingly, among the BA used in the HTPB-based CSPR, one of the most popular is tris-(2-methyl-1-aziridinyl)-phosphine oxide (MAPO, Scheme 2) whose application can be traced back to the 1950s and 1960s during the twentieth century and it is still in use today. For instance, MAPO was patented as additive for fire-proof textiles in 1959, taking the advantage of its easy ring-opening reaction of the methylaziridine rings upon modest thermal treatments [26]. Similarly, the analogous tris-(aziridinyl)-phosphine oxide (APO), also known as tris-(ethylenimine)-phosporamide (TEPA) (see structure in Scheme 3), was also used for the same purposes as MAPO [27]. The use of MAPO in CSRP can be found for instance in a patent dated 1963 [28]. The adoption of MAPO and seldom other phosphoramides as bonding agents rely on their high dipole moment, specific interaction with the oxidant of the SRP, and also for their ring-opening polymerization and crosslinking tendency which is able to encapsulate the AP particles [6,29]. It is worth remembering here that AP is a high polar ionic solid compound. For instance, silver perchlorate has a dipole moment of 11–12 D [30]. It is not known to us the dipole moment of AP, but considerations on the dipole moments of other halides and perchlorates of the first group of the Periodic Table of the Elements has led us to estimate a $\mu \approx 15$–16 D for AP. The rough reasoning was as follows: on passing from AgCl ($\mu = 6.08$ D) [31] to $AgClO_4$ ($\mu = 11.9$ D) [30] $\Delta\mu = +5.8$ D. Considering that the ammonium ionic radius is reported at 1.43 Å, closer to that of K^+ and Rb^+ (respectively 1.37 Å and 1.52 Å) [31] and known that KCl and RbCl dipole moments are respectively 10.2 and 10.5 D [31], then for NH_4ClO_4 it is expected $\mu \approx 15 - 16$ D.



Scheme 3. (From **left** to **right**) Tris-(aziridinyl)-phosphine oxide (APO) also known as tris-(ethylenimine)-phosporamide (TEPA); the sulfur analogous of TEPA known as ThioTEPA (1,1′,1″-phosphorothioyltriaziridine) and the sulfur analogous of MAPO called MethioMAPO (1,1′,1″-Phosphoryltris-(2-methylaziridine) or also tris-(methylaziridinyl)-phosphine oxide) and HMPA (Hexamethyl phosphoric acid triamide).

However, there are also drawbacks in the use of MAPO, which span from processing problems in certain SRP formulations [25], to its high toxicity [28]. Indeed, the search for other BA as substitutes of MAPO, it is supported also by the patent literature since long [29].

Regarding the MAPO toxicity, the Merck Index [32] reports that it is a chemical sterilant for living organisms with the LD_{50} = 136 mg/kg (per os) in male mice, LD_{50} = 213 mg/kg (per os) in female mice, while LD_{50} = 183 mg/kg from skin absorption in mice. Furthermore, the Merck-Aldrich safety data sheet on MAPO, reports that it is a suspect carcinogen in humans (Cat 3) and carcinogen in animals (Cat 2) [33].

From these premises, our research aimed to derive a safer BA than MAPO. Initially our interest focused on other phosphoramides [24]. Scheme 3 shows some of the selected phosphoramides of our initial interest. First of all, APO or TEPA has the same chemical structure as MAPO but the difference is represented by the aziridine rings in place of methylaziridine rings (Scheme 3). TEPA is characterized by a high dipole moment 3.5 D [21], probably similar to that of MAPO, and it is high toxic with LD_{50} = 37 mg/kg (per os) in mice and it is used as well in chemotherapy as antineoplastic [34]. Furthermore, ThioTEPA [35] and MethioTEPA (see Scheme 3) present the same toxicity problems as the corresponding TEPA and MAPO since in vivo are oxidized to the latter two compounds respectively [35]. Indeed, especially ThioTEPA it is still used as antineoplastic [34,35]. Another drawback of ThioTEPA and MethioTEPA regards the very high surface tension, 77.8 and 57.7 dyne/cm, respectively, in comparison to TEPA with 63.5 dyne/cm and MAPO with only 48.8 dyne/cm [33] which reduces considerably their ability to wet and adsorb on the AP particles. In conclusion, TEPA, ThioTEPA, and MethioTEPA, were not considered for further studies as potential BA.

Another well-known and easily accessible phosphoramide is the hexamethylphosphamide (HMPA or HMPT, see Scheme 3) which shows a series of properties somewhat similar to those of MAPO. For instance, the surface tension of HMPA is 34.4 dyne/cm, even lower than that of MAPO (48.8 dyne/cm) [33]. Furthermore, in terms of dipole moment, as summarized in Table 1, HMPA has μ = 5.5 D in bulk and 4.35 D in benzene, values much higher than 3.5 D reported for MAPO. Indeed, the $E_T(30)$ value in the Reichardt's scale also suggests a similar polarity with 41.4 kcal/mol measured in this work for MAPO, against the tabulated value of 40.9 kcal/mol for HMPA. However, HMPA has the drawback of being carcinogenic in animals and a suspected carcinogen for humans [36]. Thus, HMPA was also not considered further in this study.

To remain in the field of phosphoramides, our interest was attracted by the tris-(pyrrolidine)-phosphoramide or phosphine oxide (TTPT or TPPT) whose structure is shown in Scheme 2. First of all, this molecule appears completely safe based on the safety data sheet from Merck [37]. Furthermore, it does not present the tendency to undergo ring-opening polymerization as in the case of the aziridine, methylaziridine (three membered rings),

and azetidine rings (four membered ring). As already discussed previously [24], the ring-opening polymerization tendency of small rings in general is essentially driven by the strain energy of the ring. Thus, aziridine is highly strained and the strain energy of 27.1 kcal/mol is released during the ring-opening polymerization [38]. For the higher homologue azetidine the ring strain energy can be estimated around 20 kcal/mol as released during the ring opening reaction, using the Van Krevelen's group increment calculations [39]. However, for pyrrolidine (five-membered heterocycle), the strain energy is minimal, around 5 kcal/mol [38,39] and the ring-opening reaction is not thermodynamically allowed and the same reasoning also applies to piperidine (six-membered heterocycle) whose strain energy is nearly zero with no tendency at all to polymerize with the ring-opening mechanism. Now, the toxicity and other processing drawbacks of the phosphoramides derivatives of aziridine, methylaziridine, and azetidine are linked to the ring-opening tendency especially by the action of Lewis acids and also in other conditions [24,36]. To overcome these drawbacks, the first suitable member of the heterocyclic series is pyrrolidine and its phosphoramide derivative TTPT, shown in Scheme 2. It must be emphasized that the mechanism of action of TTPT with AP oxidizer filler will certainly be different than that of MAPO, since the ring-opening polymerization and coating of the AP granule will not occur with TTPT. Thus, the latter will act as a true plasticizer adsorbing as a liquid around the AP particles, substantially in a similar way as the conventional BA TEPAN.

As shown in Table 1, the candidate TTPT shows a considerably higher polarity either in the $E_T(30)$ scale with 52.6 kcal/mol with respect to 41.4 kcal/mol of MAPO as measured by us (see Table 1). These results with Reichardt's scale are corroborated by the high dipole moment of TTPT measured at 7.3 D in bulk and at 5.52 D in benzene [20], considerably higher than that of MAPO observed at 3.5 D. Even the dielectric constant of TTPT results are much higher than that of MAPO [45.1 vs. 14.6, respectively, see Table 1]. From these data it is definitively demonstrated that MAPO (and APO) do not have any especially high polarities and any especially high donicities [24,25]. The unicity of MAPO as a BA regarding its mechanism of action with AP has been summarized by other authors [6] and definitely involves the ring-opening polymerization mechanism on the AP surface. Regarding TTPT, the lack of ring opening polymerization is certainly compensated by the higher $E_T(30)$, μ and ε values with respect to MAPO.

In addition to TTPT as new candidate BA, we also considered a selection of alkylphosphates shown in Scheme 2. The phosphates may resemble the phosphoramides with the substitution of nitrogen atoms with oxygen and are all characterized by $\mu > 3$ D (see Table 1). In general, phosphates are indeed used as plasticizers for plastics and rubbers and are also used as special selective solvents for certain electrolytes. Reichardt's E_T (30) scale shows that TMP with 43.6 kcal/mol and TCEP with nearly similar values are very close to the conventional BA polyamine called TEPAN (see Scheme 1). On the other hand, TEP shows an $E_T(30)$ value of 41.2 kcal/mol closer to the conventional BA named K54 (see Table 1). TBUOP in its turn is closer to MAPO in the $E_T(30)$ scale (41.1 vs. 41.4 kcal/mol, respectively). Only TPP and TBP, being composed of long aliphatic chains have lower values in the $E_T(30)$ scale. Based on these results, it would be worth evaluating TMP and TCEP as replacements of TEPAN, TEP as a replacement of K54, and TBUOP as a potential replacement of MAPO in a CSRP. However, for the time being it was decided to give preference to potential BA which are characterized by very high $E_T(30)$ values, i.e., TTPT and TEA as shown in Figure 5.

As shown in Table 1, it turned out that the alcohol–amine BA called TEA (see Scheme 2 for structure) showed the highest $E_T(30)$ value with 53.5 kcal/mol among the selected liquids, although previous measurements suggested a slightly lower $E_T(30)$ value of 49.6 kcal/mol [10,11]. TEA was followed by BIFA (or HX752) in the $E_T(30)$ scale and TTPT was just in the middle between these two BA. BIFA is also an azirdinyl derivative as shown in Scheme 2. Consequently, its mechanism of interaction with AP may be similar to MAPO.

In the results section, the rationale behind the selection of TTPT and TEA to be tested as BA in a standard CSRP was already explained. Essentially, the selection fell on two potential BA characterized by high $E_T(30)$ values (among the liquids considered here). The phosphates were excluded this time from the evaluation because of a restricted number of CSRP compounds scheduled. As reference, MAPO was used because it is a universal reference BA in CSRP compounds with its special mechanism of interaction with AP, while TEPAN was selected because it is a polyamine with relatively high $E_T(30)$ value but the mechanism of interaction with AP was definitely different with respect to MAPO.

The results of CSRP mechanical properties evaluation reported in Figure 5 suggest that the selection of TTPT was really successful. Because of its high polarity, it is able to compensate the MAPO ring-opening polymerization over AP granules probably with an excellent AP–TTPT dipolar interaction which may recall solvation. After all, AP is fully soluble either in MAPO or in TTPT at room temperature [40]. The results in Figure 5 show that TTPT is able to match in full the CSRP mechanical properties of MAPO both in terms of tensile strength and elongation at break. On the other hand, TEPAN and TEA are instead able to supply higher elongation at break to the CSRP compound at the expenses of a relatively lower tensile strength.

Another interesting result of this work is the correlation that was found between the $E_T(30)$ value measured on the current and potential BA and the elongation at break (Σ) of the CSRP. Such a reasonable correlation is shown in Figure 6 and the experimental data of Figure 5 regarding Σ of CSRP were linked to the $E_T(30)$ value according to the linear equation:

$$\Sigma = 2.33[E_T(30)] - 59.36 \quad (3)$$

with $R^2 = 0.448$.

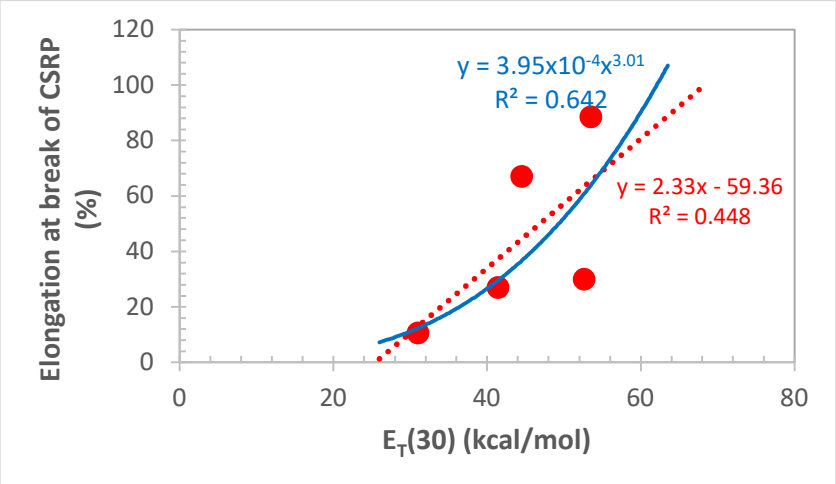


Figure 6. Correlation between the elongation at break of the CSRP (data taken from Figure 5) and $E_T(30)$ (data taken from Table 1). The experimental values can be fitted either with a linear equation with $R^2 = 0.448$ or, even better with a power law with $R^2 = 0.642$.

An even better correlation between Σ and $E_T(30)$ was found by fitting the experimental data with a power law yielding the following equation:

$$\Sigma = 3.95 \times 10^{-4}[E_T(30)]^{3.01} \quad (4)$$

with $R^2 = 0.642$.

The Σ values of CSRP were taken from Figure 5 while the $E_T(30)$ values were taken from Table 1. In Figure 6, the Σ of the reference CSRP prepared without any BA addition is also reported and the corresponding $E_T(30)$ value was taken at 31 kcal/mol since all aliphatic compounds show approximately this $E_T(30)$ value [9–11]. Since the CSRP without the BA is composed exclusively by a polybutadiene (BR) matrix filled with AP and since

polybutadiene is an aliphatic polymer, the value of $E_T(30) \approx 31$ kcal/mol was reasonably assumed as the right value for BR. After all, the unsaturated compounds n-hexene and cyclohexene have also been reported [9–11] to have $E_T(30) \approx 32$ kcal/mol, a value really close to that assigned here to BR.

5. Conclusions

MAPO is the standard bonding agent used on CSRP, but it is highly toxic to handle, and it is also too reactive. It was shown that using the Reichardt's $E_T(30)$ scale that it is possible to study the polarity of a selection of conventional liquid BA including MAPO and then, using the same $E_T(30)$ scale, new potential BA were also selected. The most remarkable new BA found in this study was TTPT which is safer than MAPO since it is not toxic, and it does not undergo hazardous polymerizations. Once tested in the CSRP compound as a substitute of MAPO, the new bonding agent TTPT was able to match in full the mechanical properties of the CSRP compounded with MAPO.

With the present work, a new dimension was added in the selection and evaluation of the BA for CSRP: the effective use of the Reichardt's $E_T(30)$ scale of polarity. The advantages offered are certainly the quick determination of the $E_T(30)$ value and, as shown in Figure 6, the reasonably good correlation of the CSRP elongation at the break with the $E_T(30)$ value of each selected BA. Indeed, it appears that higher ET(30) values of the BA, i.e., a higher polarity of the BA in the Reichardt's $E_T(30)$ scale lead to a higher elongation at the break to the CSRP composite. Furthermore, reasonable correlations between the ET(30) value and both the dielectric constant or the dipole moments of the liquids studied as BA in this study are shown in Figure S1 in Supplementary Materials.

Of course, this new approach in BA selection for CSRP does not cancel other more traditional and necessary approaches and evaluations in the selection of the BA [4–8]. The latter approaches remain absolutely valid, and are highly recommended to be applied in addition to the new one presented here.

Supplementary Materials: The following supporting information can be downloaded at: https://www.mdpi.com/article/10.3390/liquids2040017/s1.

Funding: This research received no external funding.

Data Availability Statement: Not applicable.

Conflicts of Interest: The authors declare no conflict of interest.

References

1. Mason, B.P.; Roland, C.M. Solid propellants. *Rubber Chem. Technol.* **2019**, *92*, 1–24. [CrossRef]
2. Koch, E.C. *High Explosive, Propellants, Pyrotechnics*; W. De Gruyter GmbH: Berlin, Germany, 2021.
3. Varghese, T.L.; Krishnamurthy, V.N. *The Chemistry and Technology of Solid Rocket Propellants*; Allied Publishers: New Dehli, India, 2017.
4. Lysien, K.; Stolarczyk, A.; Jarosz, T. Solid propellant formulations: A review of recent progress and utilized components. *Materials* **2021**, *14*, 6657. [CrossRef] [PubMed]
5. Cheng, T. Review of novel energetic polymers and binders–high energy propellant ingredients for the new space race. *Des. Monom. Polym.* **2019**, *22*, 54–65. [CrossRef] [PubMed]
6. Gan, J.; Zhang, X.; Zhang, W.; Hang, R.; Xie, W.; Liu, Y.; Luo, W.; Chen, Y. Research progress of bonding agents and their performance evaluation methods. *Molecules* **2022**, *27*, 340. [CrossRef] [PubMed]
7. Nguyen, T.T.; Phan, D.N.; Nguyen, D.C.; Do, V.T.; Bach, L.G. The chemical compatibility and adhesion of energetic materials with several polymers and binders: A study. *Polymers* **2018**, *10*, 1396. [CrossRef] [PubMed]
8. Naseem, H.; Yerra, J.; Murthy, H.; Ramakrishna, P.A. Ageing studies on AP/HTPB based composites solid propellants. *Energetic Mater. Front.* **2021**, *2*, 111–124.
9. Reichardt, C. *Solvents and Solvent Effects in Organic Chemistry*, 3rd ed.; Wiley-VCH: Weinheim, Germany, 2003.
10. Reichardt, C. Pyridinium-N-phenolate betaine dyes as empirical indicators of solvent polarity: Some new findings. *Pure Appl. Chem.* **2008**, *80*, 1415–1432. [CrossRef]
11. Reichardt, C.; Welton, T. *Solvents and Solvent Effects in Organic Chemistry*, 4th ed.; John Wiley & Sons: New York, NY, USA, 2011.

12. Wielgus, M.; Zaleśny, R.; Murugan, N.A.; Kongsted, J.; Ågren, H.; Samoc, M.; Bartkowiak, W. Two-photon solvatochromism ii: Experimental and theoretical study of solvent effects on the two-photon absorption spectrum of Reichardt's dye. *Chem. Phys. Chem.* **2013**, *14*, 3731–3739. [CrossRef]
13. Cerón-Carrasco, J.P.; Jacquemin, D.; Laurence, C.; Planchat, A.; Reichardt, C.; Sraïdi, K. Solvent polarity scales: Determination of new $E_T(30)$ values for 84 organic solvents. *J. Phys. Org. Chem.* **2014**, *27*, 512–518. [CrossRef]
14. Reichardt, C. Solvation effects in organic chemistry: A short historical overview. *J. Org. Chem.* **2021**, *87*, 1616–1629. [CrossRef]
15. Cataldo, F. Ozone solvatochromism in selected solvents. *J. Mol. Liq.* **2018**, *265*, 733–739. [CrossRef]
16. Mchedlov-Petrossyan, N.O.; Vodolazkaya, N.A. Protolytic equilibria in organized solutions: Ionization and tautomerism of fluorescein dyes and related indicators in cetyltrimethylammonium chloride micellar solutions at high ionic strength of the bulk phase. *Liquids* **2021**, *1*, 1–24. [CrossRef]
17. Spange, S.; Weiß, N.; Schmidt, C.H.; Schreiter, K. Reappraisal of empirical solvent polarity scales for organic solvents. *Chem.-Methods* **2021**, *1*, 42–60. [CrossRef]
18. NourEldin, A.F.; Adel, W.M.; Attai, Y.A.; Ismail, M.A. IOP Conf. *Ser. Mater. Sci. Eng.* **2020**, *973*, 012030.
19. Boshra, I.K.; Lin, G.; Elbeih, A. Influence of different crosslinking mixtures on the mechanical properties of composite solid rocket propellants based on HTPB. *High Perf. Polym.* **2021**, *33*, 52–60. [CrossRef]
20. Ozari, Y.; Jagur-Grodzinski, J. Donor strength of N-substituted phosphoramides. *J. Chem. Soc. Chem. Comm.* **1974**, *8*, 295–296. [CrossRef]
21. Bollinger, J.C.; Yvernault, G.; Yvernault, T.; Julg, A.; Rajzmann, M. Moments dipolaires et conformations de l'hexaméthylphosphotriamide (HMPT) et des dérivés aziridinylés correspondants. *J. Mol. Struct.* **1980**, *69*, 273–288. [CrossRef]
22. Diggle, J.W.; Bogsanyi, D. Physical properties and electrochemical stability of the thio solvents dimethylthioformamide and hexamethylphosphorothioic triamide. *J. Phys. Chem.* **1974**, *78*, 1018–1020. [CrossRef]
23. Dean, J.A. *Lange's Handbook of Chemistry*, 15th ed.; McGraw-Hill: New York, NY, USA, 1999.
24. Cataldo, F. A revision of the Gutmann donor numbers of a series of phosphoramides including TEPA. *Eur. Chem. Bull.* **2015**, *4*, 92–97.
25. Gal, J.F.; Maria, P.C.; Yáñez, M.; Mó, O. On the Lewis basicity of phosphoramides: A critical examination of their donor number through comparison of enthalpies of adduct formation with $SbCl_5$ and BF_3. *Chem. Phys. Chem* **2019**, *20*, 2566–2576. [CrossRef]
26. Chance, L.H.; Drake, G.L., Jr.; Reeves, W.A. Flame Resistant Organic Textiles and Method of Production. U.S. Patent No. 2,891,877, 23 June 1959.
27. Pearce, E. (Ed.) *Flame Retardant Polymeric Materials*; Plenum Press: New York, NY, USA, 1975.
28. Hudson, P.S.; Bice, C.C. Solid Composite Propellants Containing Aziridinyl Curing Agents. U.S. Patent No. 3,087,844, 30 April 1963.
29. Obert, A. Bonding Agents for HTPB-Type Solid Propellants. U.S. Patent No. 5,417,895, 23 May 1995.
30. McClellan, A.L. *Tables of Experimental Dipole Moments*; W.H. Freeman and Co., Ltd.: San Francisco, CA, USA, 1963; p. 9.
31. Lide, D.R. (Ed.) *CRC Handbook of Chemistry and Physics*; CRC Press, Taylor & Francis Group: Boca Raton, FL, USA, 2005.
32. O'Neal, M.J. (Ed.) *Merck Index*, 14th ed.; paragraph 5936; Merck Research Laboratories: Whitehouse Station, NJ, USA, 2006.
33. Data from Chemspider Website. Available online: http://www.chemspider.com/ (accessed on 4 August 2022).
34. O'Neal, M.J. (Ed.) *Merck Index*, 14th ed.; paragraph 9672; Merck Research Laboratories: Whitehouse Station, NJ, USA, 2006.
35. O'Neal, M.J. (Ed.) *Merck Index*, 14th ed.; paragraph 9673; Merck Research Laboratories: Whitehouse Station, NJ, USA, 2006.
36. Heath, D.F. *Organophosphorus Poisons Anticholinesterases and Related Compounds*; Pergamon Press: Oxford, UK, 1961.
37. TTPT Safety Data Sheet from Merck Website. Available online: https://www.sigmaaldrich.com/IT/en/sds/aldrich/93404 (accessed on 2 August 2022).
38. Cox, J.D.; Pilcher, G. *Thermochemistry of Organic and Organometallic Compounds*; Academic Press: London, UK, 1970; p. 574.
39. Van Krevelen, D.W. *Properties of Polymers: Their Correlation with Chemical Structure; Their Numerical Estimation and Prediction from Additive Group Contributions*; Elsevier: Amsterdam, The Netherlands, 1990; Chapter 20.
40. Cataldo, F. Actinium Chemical Research, Rome, Italy. **2015**, *unpublished work*.